SPINK7 Expression Changes Accompanied by HER2, P53 and RB1 Can Be Relevant to Predict Oral Squamous Cell Carcinoma at Molecular Level

Gina Pennacchiotti
Area Medicina Oral Departamento de Patología Facultad de Odontología Universidad de Chile. Av. Olivos 243, Independencia, RM CP8320000

Fabio Valdés Garrido
Instituto Nacional del Cáncer. Av. Profesor Zañartu 1010, Independencia, RM CP8320000.

Wilfredo González-Arriagada
CIICOM, Facultad de Odontología, Universidad de Valparaíso. Av. Altamirano Subida Carvallo 211. CP2390302

Héctor Montes
Departamento de cirugía cabeza-cuello Clínica Montes. Ituzaingo 1446, Capital, Mendoza, CP5500

Judith Parra
Servicio de Medicina Bucal (SEMEB), Facultad de Odontología, Universidad Nacional de Cuyo (FOdonto-UNCuyo). Centro Universitario CIT5500, Mendoza, CP5500

Valeria Guida
Servicio de Medicina Bucal (SEMEB), Facultad de Odontología, Universidad Nacional de Cuyo (FOdonto-UNCuyo). Centro Universitario CIT5500, Mendoza, CP5500

Silvina Gómez
Instituto de Medicina y Biología Experimental de Cuyo (IMBECU) CCT-Mendoza CONICET, Universidad Nacional de Cuyo (UNCuyo). Av. Adrián Ruiz Leal w/n, Mendoza, CP5500

Martín Guerrero-Gimenez
Instituto de Medicina y Biología Experimental de Cuyo (IMBECU) CCT-Mendoza CONICET, Universidad Nacional de Cuyo (UNCuyo). Av. Adrián Ruiz Leal w/n, Mendoza, CP5500

Juan Fernandez-Muñoz
Instituto de Medicina y Biología Experimental de Cuyo (IMBECU) CCT-Mendoza CONICET, Universidad Nacional de Cuyo (UNCuyo). Av. Adrián Ruiz Leal w/n, Mendoza, CP5500

Felipe Zopino
Instituto de Medicina y Biología Experimental de Cuyo (IMBECU) CCT-Mendoza CONICET, Universidad Nacional de Cuyo (UNCuyo). Av. Adrián Ruiz Leal w/n, Mendoza, CP5500

Rubén Carón
Instituto de Medicina y Biología Experimental de Cuyo (IMBECU) CCT-Mendoza CONICET, Universidad Nacional de Cuyo (UNCuyo). Av. Adrián Ruiz Leal w/n, Mendoza, CP5500

Marcelo Ezquer
Centro de Medicina Regenerativa (CMR), Facultad de Medicina, Universidad del Desarrollo-Clínica Alemana (FM, UDD-CAS). Av Las Condes 12.438, Lo Barnechea, CP7690000
Ricardo Fernández-Ramires
Facultad de Odontología, Universidad Mayor (UMayor). Avda Libertador Bernardo O`Higgins 2013. RM, CP8320000
Flavia Bruna (flabruna@gmail.com)
Instituto de Medicina y Biología Experimental de Cuyo (IMBECU) CCT-Mendoza CONICET, Universidad Nacional de Cuyo (UNCuyo). Av. Adrián Ruiz Leal w/n, Mendoza, CP5500

Research Article

Keywords: Oral squamous cancer, early detection, molecular biomarker, SPINK7, epithelial cells, Oral epithelial dysplasia.

Posted Date: November 30th, 2020

DOI: https://doi.org/10.21203/rs.3.rs-108017/v1

Version of Record: A version of this preprint was published at Scientific Reports on March 25th, 2021. See the published version at https://doi.org/10.1038/s41598-021-86208-z.

SPINK7 expression changes accompanied by HER2, P53 and RB1 can be relevant to predict oral squamous cell carcinoma at molecular level

Gina Pennacchiotti, DMD[1,7]; Fabio Valdés Garrido, MD[2]; Wilfredo A González-Arriagada, PhD[3]; Héctor F Montes, MD[4]; Judith MR Parra, DMD[5]; Valeria A Guida, DMD[5]; Silvina E Gómez, Bsc[6]; Martín E Guerrero-Gimenez, MD[6]; Juan M Fernandez-Muñoz, Bsc[6]; Felipe CM Zopino, PhD[6]; Rubén W Carón, PhD[6]; Marcelo E Ezquer, PhD[7]; Ricardo Fernández-Ramires, PhD[8] and Flavia A Bruna, PhD[5,6,7].

Author's details

1. Area Medicina Oral Departamento de Patología Facultad de Odontología Universidad de Chile. Av. Olivos 243, Independencia, Región Metropolitana, Santiago, Chile. CP8320000.
2. Instituto Nacional del Cáncer. Av. Profesor Zañartu 1010, Independencia, Región Metropolitana, Santiago, Chile. CP8320000.
3. CIICOM, Facultad de Odontología, Universidad de Valparaíso. Av. Altamirano Subida Carvallo 211. Valparaíso, Chile. CP2390302.
4. Departamento de cirugía cabeza-cuello Clínica Montes. Ituzaingo 1446, Capital, Mendoza, Argentina. CP5500.
5. Servicio de Medicina Bucal (SEMEB), Facultad de Odontología, Universidad Nacional de Cuyo (FOdonto-UNCuyo). Centro Universitario CIT5500, Capital, Mendoza, Argentina. CP5500.
6. Instituto de Medicina y Biología Experimental de Cuyo (IMBECU) CCT-Mendoza CONICET, Universidad Nacional de Cuyo (UNCuyo). Av. Adrián Ruiz Leal w/n, Capital, Mendoza, Argentina. CP5500.
7. Centro de Medicina Regenerativa (CMR), Facultad de Medicina, Universidad del Desarrollo-Clínica Alemana (FM, UDD-CAS). Av Las Condes 12.438, Lo Barnechea. Santiago, Chile. CP7690000.
8. Facultad de Odontología, Universidad Mayor (UMayor). Avda Libertador Bernardo O`Higgins 2013. Región Metropolitana, Santiago, Chile. CP8320000.

Corresponding author: Flavia A Bruna
Room: Laboratory of hormones and cancer biology, Instituto de Medicina y Biología Experimental de Cuyo (IMBECU) CCT-Mendoza CONICET, Universidad Nacional de Cuyo (UNCuyo).
Address: Av Adrián Ruiz Leal w/n, Mendoza Capital, Argentina
Postal code: 5500
Email: flabruna@gmail.com / fbruna@mendoza-conicet.gob.ar
Phone: +54 261 5244154

Abstract

The oral squamous cell carcinoma (OSCC) affects patients worldwide with a high morbidity rate. Changes of SPINK7 in precancerous lesions could promote oncogenesis. Our aim was to evaluate

SPINK7 as a potential molecular biomarker predictive of OSCC stages, compared with: HER2, TP53, RB1, NFKB and CYP4B1. Oral biopsies from patients with dysplasia (n=33), less invasive (n=28) and highly invasive OSCC (n=18) were used. 20 cases with a clinical suspicion but normal mucosa confirmed were the control. Gene levels of *SPINK7, P53, RB, NFKB* and *CYP4B1* were quantified by qPCR. *SPINK7* levels were correlated with a cohort of 330 patients from the TCGA. Also, SPINK7, HER2, TP53, and RB1, were evaluated by immunohistofluorescence. One-way Kruskal-Wallis test and Dunn's *post-hoc* with a $p<0.05$ significance was used to data analyze. In OSCC, *SPINK7* expression was down regulated and *P53, RB, NFKB* and *CYP4B1* were up regulated ($p<0.001$). Also, *SPINK7* was diminished in TCGA patients ($p=2.10e-6$). In less invasive OSCC, SPINK7 and HER2 proteins were decreased and TP53 and RB1 increased respect to others groups ($p<0.05$). Our results suggest that SPINK7 changes accompanied of HER2, P53 and RB1 can be used to classify the molecular stage of OSCC lesions, allowing a diagnosis to molecular and histopathological level.

Key words: Oral squamous cancer; early detection; molecular biomarker; SPINK7; epithelial cells; Oral epithelial dysplasia.

Introduction. Oral squamous cell carcinoma (OSCC) is the most common malignancy of the head and neck, with a high morbidity rate (37.8%) five years after diagnosis [1]. Despite great improvement in treatment and therapy, prognosis remains poor [2]. Furthermore, OSCC often causes dysfunctions and aesthetic disorders, and have a high incidence of cervical lymph node metastasis, worsen patients quality of life [3]. Several tumor biomarkers have been suggested as predictive for OSCC prognosis with poor outcome [4], however, specific molecular prognostic factors have only been partially identified [5]. The pattern of invasion (POI) presented by Brandwein-Gensler et al., classifies the POI in five types [6], and has been validated as an independent prognostic factor in oral cancer [7]. However, it is necessary to identify changes in proteins and genes, to improve diagnostic strategies in precancerous, invasive and metastatic stages [8].

One of the cancer hallmarks is the alteration of molecules related to cell adhesion and migration [9]. Adhesion molecules play a central role in pathogenesis and progression of malignant tumors [10]. Serine Peptidase Inhibitor, Kazal Type 7 (SPINK7, ECRG2) belongs to a family of 13 members (1-13) of proteins with inhibitory Serine Peptidase activity identified in 1998 in esophageal tissue [11]. This novel tumor suppressor gene was identified as a tumor suppressor gene by comparing normal esophageal epithelia and primary squamous cell carcinomas tissues [12,13]. It has been reported that SPINK7 inhibits tumor cells growth, promotes cell apoptosis, and inhibits cancer cell migration, invasion and metastasis *in vitro* [14,15].

The HER2, P53, RB1, NFKB and CYP4B1 genes and their proteins have been described altered in OSCC carcinogenesis [16]. The human epidermal growth factor receptors (HER/EGFR) are a family of trans membrane tyrosine kinase receptors comprising 1 to 4 (HER1-4) [17]. The overexpression of HER is involved in the development of oncogenesis, including OSCC, through regulating different cellular pathways. HER2 (also known as C-erbB-2/ERBB2/ErbB2) plays a critical role in the cell proliferation, survival, migration, angiogenesis, and metastasis through a variety of intracellular signaling cascades

such as MAPK/ERK1/2 and Pi3K/Akt [18,19]. An imbalance in these pathways can lead to permanent activation [20,21]. Studies have established a marked correlation between HER2 expression and the poor survival of OSCC patients [22]. It has been reported that the SPINKs protein family share 50% of homology to EGF molecule and can interact by binding to EGFR, activating EGFR downstream AKT signaling pathway, inducing epithelial mesenchymal transition [23]. The SPINK6 protein is secreted and act as a functional regulator of nasopharyngeal carcinoma cells metastasis through the bound to EGFR extracellular domain [23].

In cancer cells, tumor-suppressor genes like Protein 53 (TP53) and Retinoblastoma (RB1) are inactivated by mutation, deletion and methylation [24]. It is well established that TP53 is a genome guardian and plays a pivotal role in regulating the cell cycle, cellular differentiation, DNA repair, and apoptosis [25,26]. Somatic mutations in TP53 are detected in >60% of OSCC and in 10% of oral dysplasia [27]. Recently, Genome Wide Association Study data has shown that TP53 is usually mutated in papillomavirus-negative OSCC patients [28]. The TP53 mutations in OSCC (classified in low- and high-risk missense mutations) are associated with resistance to Cisplatin, distant metastasis and poor prognosis [29-31]. The overall survival of TP53-mutant OSCC patients is also markedly worse than patients with TP53 wild-type [32]. Previous studies reported that SPINK7 also participates in centrosome amplification in TP53-dependent manner and has a role in maintaining chromosome stability [33]. Other gene altered is RB1 that plays a key role in the regulation of cell cycle and differentiation. Its active form is phosphorylated (pRB1), acts a regulator at the G1-S restriction point arresting the cell cycle [34]. Mutations lead to functional pRB1 inactivation and failure of growth and tumor suppression control [35].

Another molecule altered in carcinogenesis is the Nuclear factor-κB (NFKB), this is a proinflammatory transcription factor that plays a pivotal role in initiation and progression of the cancer [36]. NFKB is constitutively activated in OSCCs and is involved in promoting the invasive characteristics [37]. Regarding the cell detoxification machinery, Cytochrome P450 enzyme family (CYP450) is one of the most important [38,39]. Their activity consists in catalyzing reactions that participate in both biosynthesis and degradation of drug metabolism and xenobiotic biotransformation pathways [40]. These enzymes can participate indirectly in the OSCC carcinogenesis through activation and detoxification of these compounds [38,40].

The Cancer Genome Atlas (TCGA) is an important tool to provide expression profiles from cancer patient samples and the associated clinical-pathological data for > 30 human cancer types [41]. However, there are few studies on genome-wide profiling of OSCC tumors.

The aim of this work was to determine if SPINK7 gene expression is associated to molecules altered in cancer p53, RB1, NFKB, CYP4B1 and HER2 as a good biomarker candidate of premalignant epithelial oral lesions and OSCC stages, having potential therapeutic applications (early detection and targeted therapies).

Results.

Study population data. Of a total of 71 Caucasian patients with oral dysplasia or OSCC were consent and enrolled in the present study. The average age was 52 years. The predominant gender

was male. Of the total of patients 30% had no smoking habits, 20% were light smokers (less than 10 cigarettes daily), 40% heavy smokers (more than 10 cigarettes daily) and a 10% did not specify if they had smoking habits. Being the most frequent tumor location the tongue ride (80%) **(Table 1).**

The oral epithelium changes among OSCC stages. To analyze epithelial changes in OSCC progression, the oral biopsies were evaluated by H&E and classified in dysplasia, less invasive and highly invasive OSCC. We found 33 cases of dysplasia, 28 cases of less invasive OSCC and 18 cases of highly invasive OSCC. In all dysplasia cases, the tissue did not show loss of basement membrane continuity or presence of epithelial cells invading the stroma, although an increase in epithelial cell layers and presence of mild leukocyte infiltrate was observed **(Figure 1A-D)**. In the OSCC groups both (less invasive and highly invasive), showed more than 5 layers of epithelial cells, hyperchromatism, cellular atypias and presence of keratin pearls, loss of continuity of the basement membrane and severe leukocyte infiltrate **(Figure 1B-C-E-F)**. In the highly invasive OSCC group, epithelial cell nests were observed in the stroma, total epithelial disorganization, keratin pearls and leucocyte infiltration severe. These results were correlated with poor prognosis **(Figure 1C)**. The inserts (black square) shown at high magnification the oral epithelium changes among the OSCC stages **(Figure 1D-F)**.

SPINK7 generate a distinctive molecular signature among the OSCC stages. To evaluate the molecular status of the biopsies among the OSCC stages, we assessed the gene expression of *SPINK7* with reported altered genes in carcinogenesis: *TP53, RB1, NFKB* and *CYP4B1* in the groups. We found *SPINK7* progressively down-regulated in oral dysplasia and OSCC groups respect to control ($p<0.001$). Regarding *TP53, RB1, NFKB* and *CYP4B1* all were upregulated in OSCC groups with respect to dysplasia and control groups ($p<0.001$). Additionally, with exception of *SPINK7*, we observed differential expression levels of the rest of the genes between less invasive OSCC and highly invasive OSCC groups (*TP53, RB1* and *NFKB* ($p<0.05$); *CYP4B1* $p<0.001$)) **(Figure 2A)**. The differences observed regarding the gene expression among the groups were correlated with a poor prognosis.

SPINK7 was down regulated in patients from TCGA. To evaluate if the *SPINK7* gene expression profile observed in our study population was reproducible with other cohort of OSCC patients, we analyzed the gene expression levels in 581 patients with OSCC from the TCGA (primary tissue) and the results were compared with normal subjects data (normal tissue) through *in silico* analysis [42]. The results were graphed as box plot comparing the gene expression of normal group (box plot blue) versus primary tumors group (box plot yellow) showing significant downregulation of *SPINK7* $p=2.10^{e-06}$ and this result was correlated with our results respect to *SPINK7* gene expression **(Figure 3A).**

SPINK7 does not show mutations according to TCGA mutation gene profile. To understand if the differential expression of *SPINK7* among the OSCC stages is related to a mutational profile, we analyzed *in silico* mutations described to date of a cohort of 329 patients from TCGA database. We identified 15 genes with differential mutations rate associated to OSCC, being gene of interest SPINK7 included in the analysis. We found that *TP53* was the gene with the highest number of mutations in the OSCC cohort, being mutated in 69% of patients **(Figure 3B)**. The most frequent type of variant was missense mutations followed by nonsense mutations, frameshift deletions, and multi

hits mutations. *TTN* gene showed a mutation rate of 34%, *FAT1* (26%), *CDKN2A* (22%), *NOTCH1* (18%), *PIK3CA* and *MUC16* (16%), *CASP8* (15%), *SYNE1* (14%), *CSMD3* and *PCL2* (13%) and finally, *KMT2D, LRP1B, DNAH5* and *FLG* genes were mutated in 12% of the patients. On the other hand, with a more stable mutational profile, we found *RB1* (mutated in 2% of the samples), *HER2, NFKB1* and *CYP4B1* (1%) of the cohort. Finally, we found that the *SPINK7* is a genomic stable gene, which showed no mutations in none of the cases analyzed **(Figure 3B)**.

SPINK7 and HER2 change differentially among the OSCC stages. It has been reported previously that SPINKs proteins can interact with HER2 receptor [43]. We evaluated the presence and abundance of SPINK7 among the different groups and its correlation with HER2 protein by confocal microscopy. We found that SPINK7(green signal) and HER2 (red signal) were significantly decreased in less invasive OSCC group compared with dysplasia and highly invasive OSCC groups ($p<0.05$). On another hand, the highly invasive OSCC group showed SPINK7 protein levels similar to dysplasia and no significant differences were found. Regarding HER2, it was found significantly reduced in less invasive OSCC compared to the other groups. Meanwhile, the highly invasive OSCC group showed a significant increase of HER2 compare to less invasive OSCC ($p<0.001$), being similar to the dysplasia group **(Figure 4A-B)**.

SPINK7 and HER2 were colocalized. Due to the overlapping of signals (yellow signal) between SPINK7 (green signal) and HER2 (red signal) in confocal microscopy we evaluated at high magnification images (120X digital zoom) through colocalization analysis. The intensity variability of both channels was statistically evaluated using Pearson's coefficient of 1 as positive result (r=0,99). Yellow versus red and green pixels were quantified yielding a co-occurrence value of 56.58% **(Figure 4C)**.

TP53 and pRB1 change differentially among the OSCC stages. To evaluate cell cycle regulators in the OSCC, we analyzed TP53 and pRB1 protein levels among the groups by confocal microscopy. The less invasive OSCC group showed a significant increase of TP53 and pRB1 compared with dysplasia and highly invasive OSCC groups ($p<0.05$). Regarding the highly invasive OSCC group, both proteins (TP53 and pRB1) significantly decreased respect to the other groups ($p<0.001$) **(figure 5A-B)**.

Discussion. The oral squamous cell carcinoma has a high morbidity rate in the world [1]. Despite the progress in research and therapy, survival has not improved significantly in the last decades [44]. The biomarkers study aims to understand the role of genetic and lifestyle factors of the tumor biology included the OSCC [45]. We studied changes in proteins related with some of the cancer hallmarks (cell survival, cell cycle, inflammation, metastasis and metabolism) to stratify molecularly oral precancerous and cancerous lesions [46]. Currently, the gold standard of OSCC diagnosis is the biopsy, however, the results are observer-dependent and subjective [44,47].

The current study is reporting the SPINK7 expression changes among the OSCC stages and we propose this protein as a "*new biomarker"* associated with the natural progression of the OSCC. We found differences among the oral epithelial organization in dysplasia and less or highly invasive OSCC groups, and these results were correlated with the literature [48,49], showing a differential gene

expression profile by qPCR analysis with a distinctive "molecular signature" in each stage. We found *SPINK7* significantly down regulated at dysplasia and OSCC compared with control group. Meanwhile *TP53, RB1, NFKB and CYP4B1* were significantly up regulated at OSCC stages compare with dysplasia and control groups. The results obtained by SPINK7 in our study population were compared with a cohort of 541 patients from the TGCA database [50]. The comparative analysis showed that *SPINK7* was significantly down regulated in patients with OSCC compare to normal tissue and this could be related with the advance grade of the malignant lesion [51]. Additionally, we analyzed the mutation profile of genes described in TCGA altered in OSCC included *SPINK7, TP53, RB1, NFKB* and *CYP4B1*. We found that *TP53* showed a high mutation rate in OSCC meanwhile *SPINK7* was the most stable without any mutation described. These results suggest that the downregulation of the gene would be related to other mechanisms, not associated to *TP53* gene, and need to be explored in a future.

Due the SPINK's protein family is related with extracellular matrix remodeling and cell migration regulation [43]. We evaluated the abundance of SPINK7 and HER2 and if there are correlation between them, because has been reported that SPINK7 shares 50% of homology with EGF [43]. We found SPINK7 up regulated in the highly invasive OSCC group, these results were similar to previous studies describing that SPINK6 was up regulated in highly metastatic tumors [43]. SPINK6 regulate the metastasis via EGFR signaling and their expression levels change during the carcinogenesis [52]. Interestingly SPINK7 and HER2 were overexpressed in the highly invasive OSCC compared with less invasive OSCC. Additionally the SPINK7 and HER2 colocalization analysis showed that both proteins are close suggesting interaction, however subsequent tests with a larger sample size are necessary to evaluate and understand its interaction or co-compartmentalization [51]. The differential expression of the studied proteins among the OSCC stages could be related with disorganization of the oral epithelium and to a non-functional protein or absence of their ligands, but it needs to be explored in more detail in the future [53]. The differential proteins expression among the stages allowed stratifying the groups to molecular and histological levels correlated with prognosis. It has been reported in esophageal cancer that cells treated with a siRNA for SPINK1 were resistant to the antitumoral drug Cisplatin [54]. This could be interesting in order to stratify the patients who respond, or not, to the standard chemotherapy.

Regarding the studied cell cycle factors, TP53 and pRB1, we found through confocal microscopy analysis that both proteins were upregulated in the less invasive OSCC respect to dysplasia; meanwhile in the highly invasive OSCC both were downregulated, which consistent with previous studies [55]. These could be explained according to the TCGA *in silico* analysis with the high rate of mutation profile that both genes showed in OSCC. These results suggest that in OSCC, TP53 and pRB1 are present but non-functional and this could be related with a more aggressive tumor [55].

Our results suggest that the changes in the expression of SPINK7 can be used to predict the molecular stage of the OSCC lesions. This molecule could be a new "potential" biomarker. Futures studies are needed to validate this novel tumor suppressor gene that could be applied as a possible early diagnostic method to precancerous oral lesions and OSCC.

Methods

Study population. Patients with suspected oral lesions of OSCC were enrolled. After signing the informed consent, the subjects were interviewed using a standard questionnaire that requested information about socio-demographic, medical, and lifestyle factors. The patients from Department of Head and Neck surgery of The National Cancer Institute, Dental school of Universidad de Valparaíso, Dental school of Universidad del Desarrollo (Chile), The Hospital Lencinas and the Servicio de Estomatología y Medicina Bucal Dental school, Universidad Nacional de Cuyo (Argentina); received a routine intraoral examination and oral mucosal biopsies were taken and classified according to the diagnosis and POI in three groups: oral epithelial dysplasia, less invasive OSCC (POI type 1 and 2) and invasive OSCC (POI type 3, 4 and 5) group. Seventy-one cases of primary OSCC diagnosed over a period of 2 years (2017–2019) were included in the study. None of the patients had received any tumor specific therapy (chemotherapy or radiotherapy) before the resection. Twenty cases diagnosed as inflammatory lesions and histologically confirmed with normal mucosal margins from the resection specimens were included as control group in the qPCR analysis. The Ethics Committee of the School of Medicine of Universidad del Desarrollo (FM-UDD CAS), National Cancer Institute of Chile and Medicine School of Universidad Nacional de Cuyo (FCM-UNCuyo) approved this study according to Declaration of Helsinki to experimentation with human subjects.

Histopathological analysis. The Oral biopsies were fixed in 10% buffered formalin (Merck, USA), embedded in paraffin (Merck), and sectioned. Tissue sections of 4 µm were deparaffinized with Neoclear (Merck), rehydrated with graded alcohols, stained with hematoxylin–eosin (H&E, Merck), and visualized with a light microscope (DM2000; Leica, Germany). Images were captured with a digital camera (DFC295; Leica). Samples were classified according to the revised criteria given by the World Health Organization (2005). Three independent observers performed histological analyses blind; one of them is a pathologist expert in oral diseases [56,57].

Immunohistofluorescence analysis. Tissue sections of 4 µm were deparaffinized, rehydrated, blocked with 5% FBS (Gibco, USA) dissolved in PBS 1X (Gibco, USA) and incubated overnight at 4 °C with a dilution 1:50 of antibodies for anti-SPINK7 (Abcam, ab122326, USA), anti-HER2 (BD Pharmigen™, #554299, USA), anti-p53 (Abcam, (PAb 1801 ab28, USA) and anti-pRB (8516S, Cell signaling, USA). Then, samples were washed with PBS 1X and incubated two hours at room temperature with a dilution 1:400 of Alexa488-conjugated goat anti-mouse IgG or Alexa 555-conjugated rabitt anti-mouse IgG (Cell Signaling, USA). Cross-reactivity of the secondary antibody was tested incubating samples without the primary antibody. Nuclei were counterstained with a dilution 1:1500 of DAPI (Sigma, Aldrich) in PBS 1X. Samples were embedded in fluorescence mounting medium S3023 (Dako cytomation, USA) and scanned in a confocal microscope (Olympus). Five representative optical sections by sample (n=6/group) were photographed using 60X magnification. The images obtained per field of each sample, were processed with the same conditions and the positive protein signal (pixels intensity) was analyzed and quantified using Fiji Image J software (NIH, USA) [56,57].

Confocal microscopy analysis A Gaussian filter of 1 was applied and a constant background value of 150 was subtracted for each image. The same threshold value was set for each channel including

the structures of interest and the corresponding masks were obtained. The yellow pixels (red and green pixels overlap) versus the total pixels were quantified and the colocalization was measured with Coloc2 plugin (Fiji ImageJ) [51].

Gene expression analysis Total RNA was isolated from the oral biopsies. The mRNA was purified using RNEasy PlusMini Kit (Qiagen, Germany). Contaminating genomic DNA was degraded with 1 U of DNAse RQ1 (Promega). One µg of RNA was reverse transcribed for 60 min at 42 °C using 200 U M-MLV reverse transcriptase (Invitrogen) and 0.5 µM oligo-dT primers (Invitrogen). Real time PCR was performed in a final volume of 10 µL containing 50 ng of cDNA, Power SYBR Green PCR master mix (Life Technologies, Grand Island, NY) and 0.5 µM of each specific primer, using the Step One Plus PCR system (Life Technologies). Controls without reverse transcriptase were included. Amplicons were analyzed according to their size and melting temperature (Supplementary Table 1, S1). To normalize data, 18S RNA and β-actin were used as reference genes. The RNA level of a target gene was calculated using the 2ΔCt method and graphed as fold change [58].

Gene expressions TCGA profile. The data studied was programmatically extracted from the publicly available data set of OSCC from The Cancer Genome Atlas Project (TCGA) on May, 2019 using the recount2 platform (https://jhubiostatistics.shinyapps.io/recount/). Non-standardized RNASeq gene expression levels from 548 samples were downloaded. Samples from oral cavity were selected obtaining a final subset of 332 tumor samples and 32 non-tumoral tissue samples. RNA expression levels were evaluated for 6 genes (NFKB1, RB1, TP53, ERBB2, CYP4B1, SPINK7). Crude counts were scaled by the total coverage of the sample (area under the curve, 'AUC') and differential gene expression analysis (DGE) was performed using the generalized linear model method of the EdgeR R package comparing non-tumor versus tumor samples [59]. Log_2 Fold change values were obtained associated with exact p-values and False Discovery Rate values (FDR). To evaluate gene expression correlation, data was transformed using Voom conversion from the R limma package, allowing normal linear modeling of the RNA counts. Afterwards, pairwise Pearson's product-moment correlation analysis was performed for the aforementioned genes and p-values were calculated [50].

Gene mutations TCGA profile. The mutational analysis of OSCC, data was programmatically downloaded using the TCGA biolinks package of Bioconductor [60]. Mutation Annotation Format (MAF) files with aggregated mutation information generated from whole-exome sequencing were downloaded. From 546 samples of Head and Neck cancer, 329 samples of OSCC were obtained. The maftools Bioconductor package was used to analyze and visualize the MAF files [61]. An Oncoplot was drawn showing the variants (SNP) of the 15 most mutated genes in OSCC, followed by 5 genes of interest (RB1, ERBB2, NFKB1, CYP4B1 and SPINK7)[50].

Statistical analysis. The population distribution of the samples from our patients was non-parametric. Comparisons of gene and protein expression among the groups were performed using One-way Kruskal-Wallis test and Dunn's test as post-test. Stat Graph Prism 5.0 software was used for statistical analysis. Data are presented as median ± SEM, and $p<0.05$ was considered statistically significative.

References:

1 Torre, L. A. *et al.* Global cancer statistics, 2012. *CA: a cancer journal for clinicians* **65**, 87-108, doi:10.3322/caac.21262 (2015).

2 Grandi, C. *et al.* Prognostic significance of lymphatic spread in head and neck carcinomas: therapeutic implications. *Head & neck surgery* **8**, 67-73 (1985).

3 Fillies, T. *et al.* Catenin expression in T1/2 carcinomas of the floor of the mouth. *International Journal of Oral and Maxillofacial Surgery* **34**, 907-911, doi:https://doi.org/10.1016/j.ijom.2005.03.010 (2005).

4 Rivera, C., Oliveira, A. K., Costa, R. A. P., De Rossi, T. & Paes Leme, A. F. Prognostic biomarkers in oral squamous cell carcinoma: A systematic review. *Oral oncology* **72**, 38-47, doi:10.1016/j.oraloncology.2017.07.003 (2017).

5 Ramaekers, F. C. *et al.* Coexpression of keratin- and vimentin-type intermediate filaments in human metastatic carcinoma cells. *Proceedings of the National Academy of Sciences of the United States of America* **80**, 2618-2622, doi:10.1073/pnas.80.9.2618 (1983).

6 Brandwein-Gensler, M. *et al.* Oral squamous cell carcinoma: histologic risk assessment, but not margin status, is strongly predictive of local disease-free and overall survival. *Am J Surg Pathol* **29**, 167-178, doi:10.1097/01.pas.0000149687.90710.21 (2005).

7 Almangush, A. *et al.* Depth of invasion, tumor budding, and worst pattern of invasion: prognostic indicators in early-stage oral tongue cancer. *Head Neck* **36**, 811-818, doi:10.1002/hed.23380 (2014).

8 Sethi, S., Ali, S., Philip, P. A. & Sarkar, F. H. Clinical advances in molecular biomarkers for cancer diagnosis and therapy. *International journal of molecular sciences* **14**, 14771-14784, doi:10.3390/ijms140714771 (2013).

9 Hanahan, D. & Weinberg, R. A. Hallmarks of cancer: the next generation. *Cell* **144**, 646-674 (2011).

10 Hanahan, D. & Weinberg, R. A. The hallmarks of cancer. *Cell* **100**, 57-70 (2000).

11 Imai, K. *et al.* Immunolocalization of desmoglein and intermediate filaments in human oral squamous cell carcinomas. *Head & neck* **17**, 204-212 (1995).

12 Cui, Y., Bi, M., Su, T., Liu, H. & Lu, S.-H. Molecular cloning and characterization of a novel esophageal cancer related gene. *International journal of oncology* **37**, 1521-1528 (2010).

13 Su, T., Liu, H. & Lu, S. Cloning and identification of cDNA fragments related to human esophageal cancer. *Zhonghua zhong liu za zhi [Chinese journal of oncology]* **20**, 254-257 (1998).

14 Chui, X. *et al.* Immunohistochemical expression of the c-kit proto-oncogene product in human malignant and non-malignant breast tissues. *British journal of cancer* **73**, 1233-1236, doi:10.1038/bjc.1996.236 (1996).

15 Engels, K. *et al.* Dynamic intracellular survivin in oral squamous cell carcinoma: underlying molecular mechanism and potential as an early prognostic marker. *The Journal of pathology* **211**, 532-540, doi:10.1002/path.2134 (2007).

16 Clevers, H. Wnt/beta-catenin signaling in development and disease. *Cell* **127**, 469-480, doi:10.1016/j.cell.2006.10.018 (2006).

17 Bernardes, V. F., Gleber-Netto, F. O., Sousa, S. F., Silva, T. A. & Aguiar, M. C. Clinical significance of EGFR, Her-2 and EGF in oral squamous cell carcinoma: a case control study. *Journal of experimental & clinical cancer research : CR* **29**, 40, doi:10.1186/1756-9966-29-40 (2010).

18 Press, M. F. & Lenz, H. J. EGFR, HER2 and VEGF pathways: validated targets for cancer treatment. *Drugs* **67**, 2045-2075, doi:10.2165/00003495-200767140-00006 (2007).

19 Burgess, A. W. *et al.* An open-and-shut case? Recent insights into the activation of EGF/ErbB receptors. *Molecular cell* **12**, 541-552, doi:10.1016/s1097-2765(03)00350-2 (2003).

20 Feng, Y. *et al.* Breast cancer development and progression: Risk factors, cancer stem cells, signaling pathways, genomics, and molecular pathogenesis. *Genes Dis* **5**, 77-106, doi:10.1016/j.gendis.2018.05.001 (2018).

21 Bernardes, V. F., Gleber-Netto, F. O., Sousa, S. F., Silva, T. A. & Aguiar, M. C. F. Clinical significance of EGFR, Her-2 and EGF in oral squamous cell carcinoma: a case control study. *Journal of Experimental & Clinical Cancer Research* **29**, 40, doi:10.1186/1756-9966-29-40 (2010).

22 Sasahira, T. & Kirita, T. Hallmarks of Cancer-Related Newly Prognostic Factors of Oral Squamous Cell Carcinoma. *International journal of molecular sciences* **19**, doi:10.3390/ijms19082413 (2018).

23 Zheng, L.-S. *et al.* SPINK6 promotes metastasis of nasopharyngeal carcinoma via binding and activation of epithelial growth factor receptor. *Cancer research* (2016).

24 Kim, M. S., Li, S. L., Bertolami, C. N., Cherrick, H. M. & Park, N. H. State of p53, Rb and DCC tumor suppressor genes in human oral cancer cell lines. *Anticancer research* **13**, 1405-1413 (1993).

25 Choi, S. & Myers, J. Molecular pathogenesis of oral squamous cell carcinoma: implications for therapy. *Journal of dental research* **87**, 14-32 (2008).

26 Daniela Adorno-Farias, J. P. A., Montserrat Reyes, Ana Ortega, Blanca Urzúa, Lilian Jara, Alfredo Molina, José Jara, Jean Nunes dos Santos, Sandra Tarquínio, Ricardo Fernández-Ramires. Alteraciones genéticas de la mucosa oral hacia la transformación maligna. *Acta Odontologica Venezolana* **55** (2017).

27 Hanahan, D. & Weinberg, R. A. Hallmarks of cancer: the next generation. *Cell* **144**, 646-674, doi:10.1016/j.cell.2011.02.013 (2011).

28 Network, C. G. A. Comprehensive genomic characterization of head and neck squamous cell carcinomas. *Nature* **517**, 576-582, doi:10.1038/nature14129 (2015).

29 Neskey, D. M. *et al.* Evolutionary Action Score of TP53 Identifies High-Risk Mutations Associated with Decreased Survival and Increased Distant Metastases in Head and Neck Cancer. *Cancer research* **75**, 1527-1536, doi:10.1158/0008-5472.can-14-2735 (2015).

30 Osman, A. A. *et al.* Evolutionary Action Score of TP53 Coding Variants Is Predictive of Platinum Response in Head and Neck Cancer Patients. *Cancer research* **75**, 1205-1215, doi:10.1158/0008-5472.can-14-2729 (2015).

31 Sandulache, V. C. *et al.* High-Risk TP53 Mutations Are Associated with Extranodal Extension in Oral Cavity Squamous Cell Carcinoma. *Clinical cancer research : an official journal of the American Association for Cancer Research* **24**, 1727-1733, doi:10.1158/1078-0432.ccr-17-0721 (2018).

32 de Oliveira, L. R., Ribeiro-Silva, A. & Zucoloto, S. Prognostic impact of p53 and p63 immunoexpression in oral squamous cell carcinoma. *Journal of oral pathology & medicine : official publication of the International Association of Oral Pathologists and the American Academy of Oral Pathology* **36**, 191-197, doi:10.1111/j.1600-0714.2007.00517.x (2007).

33 Cheng, X., Shen, Z., Yang, J., Lu, S.-H. & Cui, Y. ECRG2 disruption leads to centrosome amplification and spindle checkpoint defects contributing chromosome instability. *Journal of Biological Chemistry* **283**, 5888-5898 (2008).

34 Thomas, S., Balan, A. & Balaram, P. The expression of retinoblastoma tumor suppressor protein in oral cancers and precancers: A clinicopathological study. *Dent Res J (Isfahan)* **12**, 307-314, doi:10.4103/1735-3327.161427 (2015).

35 Pande, P., Mathur, M., Shukla, N. K. & Ralhan, R. pRb and p16 protein alterations in human oral tumorigenesis. *Oral oncology* **34**, 396-403, doi:10.1016/s1368-8375(98)00024-4 (1998).

36 Postler, T. S. & Ghosh, S. Bridging the gap: A regulator of NF-κB linking inflammation and cancer. *Journal of Oral Biosciences* **57**, 143-147, doi:https://doi.org/10.1016/j.job.2015.05.001 (2015).

37 Jimi, E. *et al.* NF-κB acts as a multifunctional modulator in bone invasion by oral squamous cell carcinoma. *Oral Science International* **13**, 1-6, doi:https://doi.org/10.1016/S1348-8643(15)00038-5 (2016).

38 Xu, X., Zhang, X. A. & Wang, D. W. The roles of CYP450 epoxygenases and metabolites, epoxyeicosatrienoic acids, in cardiovascular and malignant diseases. *Adv Drug Deliv Rev* **63**, 597-609, doi:10.1016/j.addr.2011.03.006 (2011).

39 Zelasko, S., Arnold, W. R. & Das, A. Endocannabinoid metabolism by cytochrome P450 monooxygenases. *Prostaglandins Other Lipid Mediat* **116-117**, 112-123, doi:10.1016/j.prostaglandins.2014.11.002 (2015).

40 Pikuleva, I. A. & Waterman, M. R. Cytochromes p450: roles in diseases. *The Journal of biological chemistry* **288**, 17091-17098, doi:10.1074/jbc.R112.431916 (2013).

41 Sundaram, K., Sambandam, Y., Tsuruga, E., Wagner, C. L. & Reddy, S. V. 1α,25-dihydroxyvitamin D3 modulates CYP2R1 gene expression in human oral squamous cell carcinoma tumor cells. *Horm Cancer* **5**, 90-97, doi:10.1007/s12672-014-0170-5 (2014).

42 Creighton, C. J. Making Use of Cancer Genomic Databases. *Curr Protoc Mol Biol* **121**, 19.14.11-19.14.13, doi:10.1002/cpmb.49 (2018).

43 Zheng, L.-S. *et al.* SPINK6 Promotes Metastasis of Nasopharyngeal Carcinoma via Binding and Activation of Epithelial Growth Factor Receptor. *Cancer research* **77**, 579-589, doi:10.1158/0008-5472.CAN-16-1281 (2017).

44 Woolgar, J. A. & Triantafyllou, A. Pitfalls and procedures in the histopathological diagnosis of oral and oropharyngeal squamous cell carcinoma and a review of the role of pathology in prognosis. *Oral oncology* **45**, 361-385 (2009).

45 Cervino, G. *et al.* Molecular Biomarkers Related to Oral Carcinoma: Clinical Trial Outcome Evaluation in a Literature Review. *Disease markers* **2019**, 8040361, doi:10.1155/2019/8040361 (2019).

46 Williams, H. K. Molecular pathogenesis of oral squamous carcinoma. *Molecular Pathology* **53**, 165-172 (2000).

47 Zini, A., Czerninski, R. & Sgan‐Cohen, H. D. Oral cancer over four decades: epidemiology, trends, histology, and survival by anatomical sites. *Journal of oral pathology & medicine* **39**, 299-305 (2010).
48 Napier, S. S. & Speight, P. M. Natural history of potentially malignant oral lesions and conditions: an overview of the literature. *Journal of oral pathology & medicine* **37**, 1-10 (2008).
49 Speight, P. M. & Farthing, P. M. The pathology of oral cancer. *British Dental Journal* **225**, 841-847, doi:10.1038/sj.bdj.2018.926 (2018).
50 Zoppino, F. C. M., Guerrero-Gimenez, M. E., Castro, G. N. & Ciocca, D. R. Comprehensive transcriptomic analysis of heat shock proteins in the molecular subtypes of human breast cancer. *BMC cancer* **18**, 700-700, doi:10.1186/s12885-018-4621-1 (2018).
51 Moser, B., Hochreiter, B., Herbst, R. & Schmid, J. A. Fluorescence colocalization microscopy analysis can be improved by combining object-recognition with pixel-intensity-correlation. *Biotechnol J* **12**, 1600332, doi:10.1002/biot.201600332 (2017).
52 Vats, S., Ganesh, M. & Agarwal, A. Human epidermal growth factor receptor 2 neu expression in head and neck squamous cell cancers and its clinicopathological correlation: Results from an Indian cancer center. *Indian Journal of Pathology and Microbiology* **61**, 313-318, doi:10.4103/0377-4929.236599 (2018).
53 Mazzoccoli, G. *et al.* A primary tumor gene expression signature identifies a crucial role played by tumor stroma myofibroblasts in lymph node involvement in oral squamous cell carcinoma. *Oncotarget* **8** (2017).
54 Goldstein, A. S., Zong, Y. & Witte, O. N. A Two-Step Toward Personalized Therapies for Prostate Cancer. *Science Translational Medicine* **3**, 72ps77, doi:10.1126/scitranslmed.3002169 (2011).
55 Lakshminarayana, S. *et al.* Molecular pathways of oral cancer that predict prognosis and survival: A systematic review. *J Carcinog* **17**, 7-7, doi:10.4103/jcar.JCar_17_18 (2018).
56 Bruna, F., Arango-Rodríguez, M., Plaza, A., Espinoza, I. & Conget, P. The administration of multipotent stromal cells at precancerous stage precludes tumor growth and epithelial dedifferentiation of oral squamous cell carcinoma. *Stem Cell Research* **18**, 5-13, doi:https://doi.org/10.1016/j.scr.2016.11.016 (2017).
57 Bruna, F., Plaza, A., Arango, M., Espinoza, I. & Conget, P. Systemically administered allogeneic mesenchymal stem cells do not aggravate the progression of precancerous lesions: a new biosafety insight. *Stem Cell Research & Therapy* **9**, 137 (2018).
58 Schmittgen, T. D. & Livak, K. J. Analyzing real-time PCR data by the comparative CT method. *Nature Protocols* **3**, 1101-1108, doi:10.1038/nprot.2008.73 (2008).
59 Wang, T., Li, B., Nelson, C. E. & Nabavi, S. Comparative analysis of differential gene expression analysis tools for single-cell RNA sequencing data. *BMC Bioinformatics* **20**, 40-40, doi:10.1186/s12859-019-2599-6 (2019).
60 Colaprico, A. *et al.* TCGAbiolinks: an R/Bioconductor package for integrative analysis of TCGA data. *Nucleic acids research* **44**, e71-e71, doi:10.1093/nar/gkv1507 (2016).
61 Mayakonda, A., Lin, D.-C., Assenov, Y., Plass, C. & Koeffler, H. P. Maftools: efficient and comprehensive analysis of somatic variants in cancer. *Genome Res* **28**, 1747-1756, doi:10.1101/gr.239244.118 (2018).

Acknowledgments. To Instituto Nacional del Cancer Chile; CIICOM; Clínica Montes; SEMEB, UNCuyo; IMBECU CCT-Mendoza CONICET; CMR, UDD-CAS; Facultad de Odontología, UMayor.

Author's contributions. The authors of the present work have made substantial contribution to the article. RFR and FAB contributed to the conception and design of the work. FAB wrote the main manuscript text. GP, FVG, WAGA, HFM, JMRP, VAG, SEG, RFR and FAB contributed to the acquisition, analysis and interpretation of data obtained from patient's biopsies. RFR and FAB prepared figures 1-2; 4-5. MEGG, JMFM and FCMZ contributed to the database acquisition, in silico analysis and interpretation of TGCA data obtained from the USA Cancer Atlas and prepared the figure 3. RFR, FAB, MEE and RWC contributed with the discussion section.

All the authors reviewed the manuscript.

Funding

This work was supported by: PI UDD-CAS N20141001185304708249 grant (FAB); Foundation JA Roemmers (FAB) and Project FDP Universidad Mayor RFR (PEP I-2019081) (RFR).

Ethics approval and consent to participate

The Ethics Committee of the School of Medicine of Universidad del Desarrollo (FM-UDD CAS), National Cancer Institute of Chile and Medicine School of Universidad Nacional de Cuyo (FCM-UNCuyo) approved this study according to Declaration of Helsinki to experimentation with human subjects.

Conflict of interest

The authors declare that they have no competing interests.

Tables

Population of study data	Number of Patients with OSCC lesions (n)	Percentage of Patients with OSCC lesions (%)
Age		
< 40 years old	12	15%
41-59 years old	32	40%
>60 years old	37	45%
Gender		
Female	32	40%
Male	49	60%
Smoke habits		
No	24	30%
Light smokers (<5/día)	16	20%
Heavy smokers (>10/día)	41	40%
Non specific	1	10%

Table 1. Socio-demographics data of study population

Figures & legends

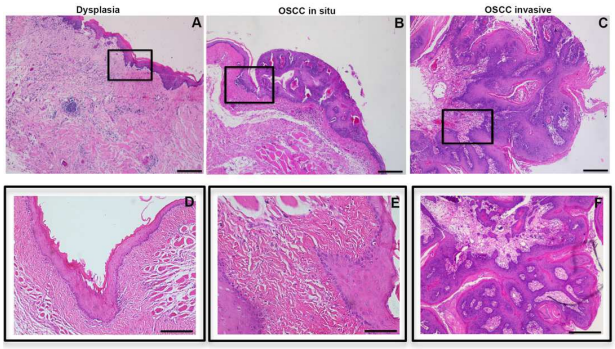

Figure 1. OSCC stages H&E analysis. Oral biopsies of patients were analyzed by H&E and classified into dysplasia (Figures 1A and 1D), less invasive OSCC (Figures 1B and 1E) and highly invasive OSCC (Figures 1C and 1F) according to the changes in the epithelium.

The Figures 1A and 1D shown that in all dysplasia cases at different magnification. Regarding the tissue did not show loss of basal membrane continuity or presence of epithelial cells invading the stroma, although an increase in epithelial cell layers and presence of mild leukocyte infiltrate was observed.

The biopsies of patients with OSCC both less (Figures 1B and 1 E) and highly invasive cases (Figures 1C and 1F), showed at different magnification more than 5 layers of epithelial cells, hyperchromatism, presence of keratin pearls, loss of continuity of the basement membrane and severe leukocyte infiltrate were seen. In the highly invasive OSCC group, epithelial cell nests were observed in the stroma and severe epithelium disorganization, accompanied of leucocyte infiltration of high grade (Figures 1C-F).

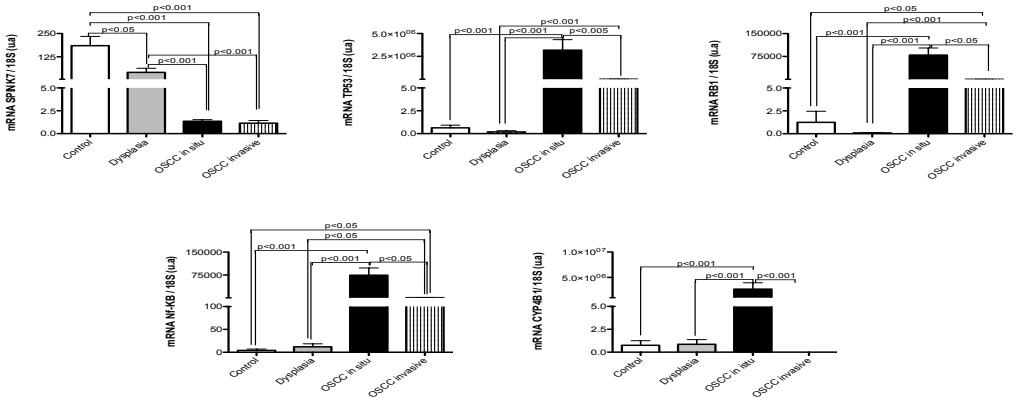

Figure 2. *SPINK7, TP53, RB1, NFKB* and *CYP4B1* gene expression change among the OSCC stages. The graph bar showed the gene expression evaluated by qPCR of each group (normal, dysplasia, less invasive and highly invasive OSCC) and the results were expressed as arbitrary units. The differences were considered statistically significance with *P* values of (**P*<0.05, ***P*<0.01 and ****P*<0.001).

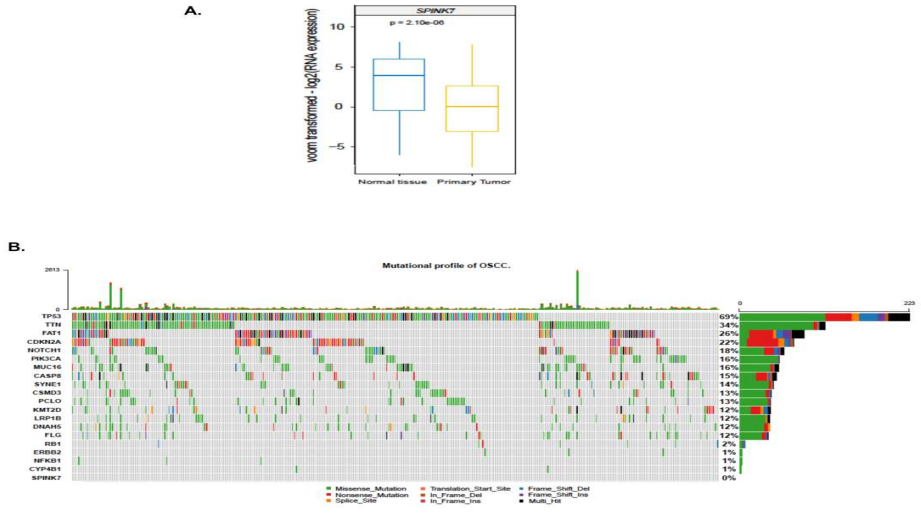

Figure 3. *SPINK7* gene expression and mutational profile in a cohort of patients from the TCGA database. A) Box-plot derived of TCGA gene expression analysis of *SPINK7* from 581 samples of normal group (box-plot blue) vs primary tumors group (box-plot yellow). B) The Oncoplot graph shows the profile of oral cancer mutations taking into account the fifteen genes with the highest number of mutations (SNP) followed by five genes of interest (*RB1, ERBB2/HER2, NFKB1, CYP4B1* and *SPINK7*). Each column represents a sample of oral cancer and each color represents a type of mutation variant. On the right, the size of each bar represents the frequency of mutations throughout

all samples and the percentage of samples that have this mutated gene. Variants annotated as Multi_Hit are those genes that are mutated more than once in the same sample. In the upper part the number of mutations that each sample has graphed.

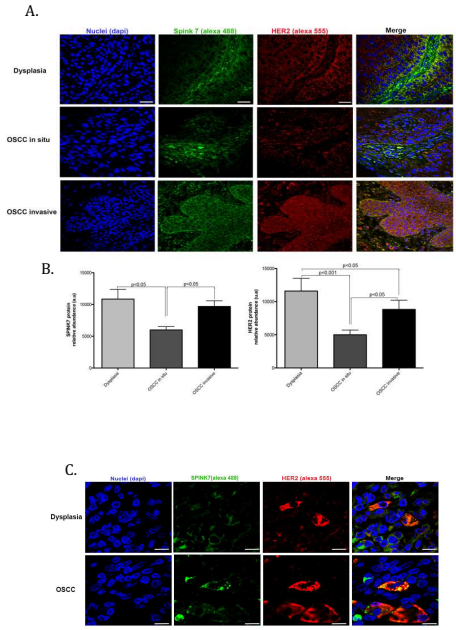

Figure 4. SPINK7 and HER2 proteins analysis among the OSCC stages. A) Immunohistofluorescence of SPINK7 (green) and HER2 (red) proteins evaluated in biopsies of dysplasia, less invasive and highly invasive OSCC. Nuclei were stained with Dapi (blue).
The Figure 4B show the graphs bar of the quantitative analysis of pixels intensity (green=SPINK7 and red=HER2) assessed by Image J.
The Figure 4C) show the images at high magnification (120X) among the OSCC stages, showing the close localization of both proteins' signals through overlap image (yellow pixels), Representative images by group, n=6. White bar = 50 µm. The differences were considered statistically significance with *P* values of (**P*<0.05 and ****P*<0.001).

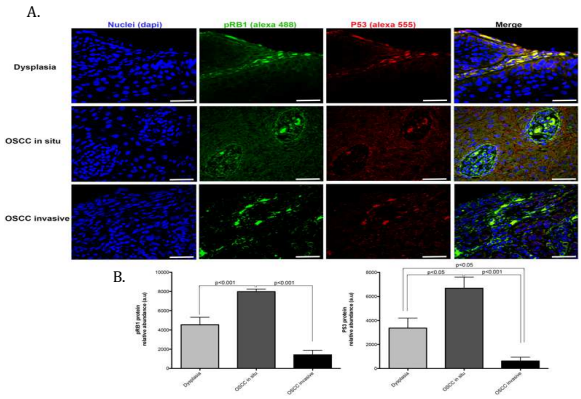

Figure 5. pRB1 and P53 proteins analysis among the OSCC stages. A) Immunohistofluorescence of both proteins, evaluated in biopsies of dysplasia, less invasive and highly invasive OSCC. B)

573 Graphs bar show quantitative analysis of pixels intensity (green=pRB1 and red=P53) assessed by
574 ImageJ. Representative images by group, n=6/group. White bar = 50 μm. The differences were
575 considered statistically significance with *P* values of (*$P<0.05$ and ***$P<0.001$).

Figures

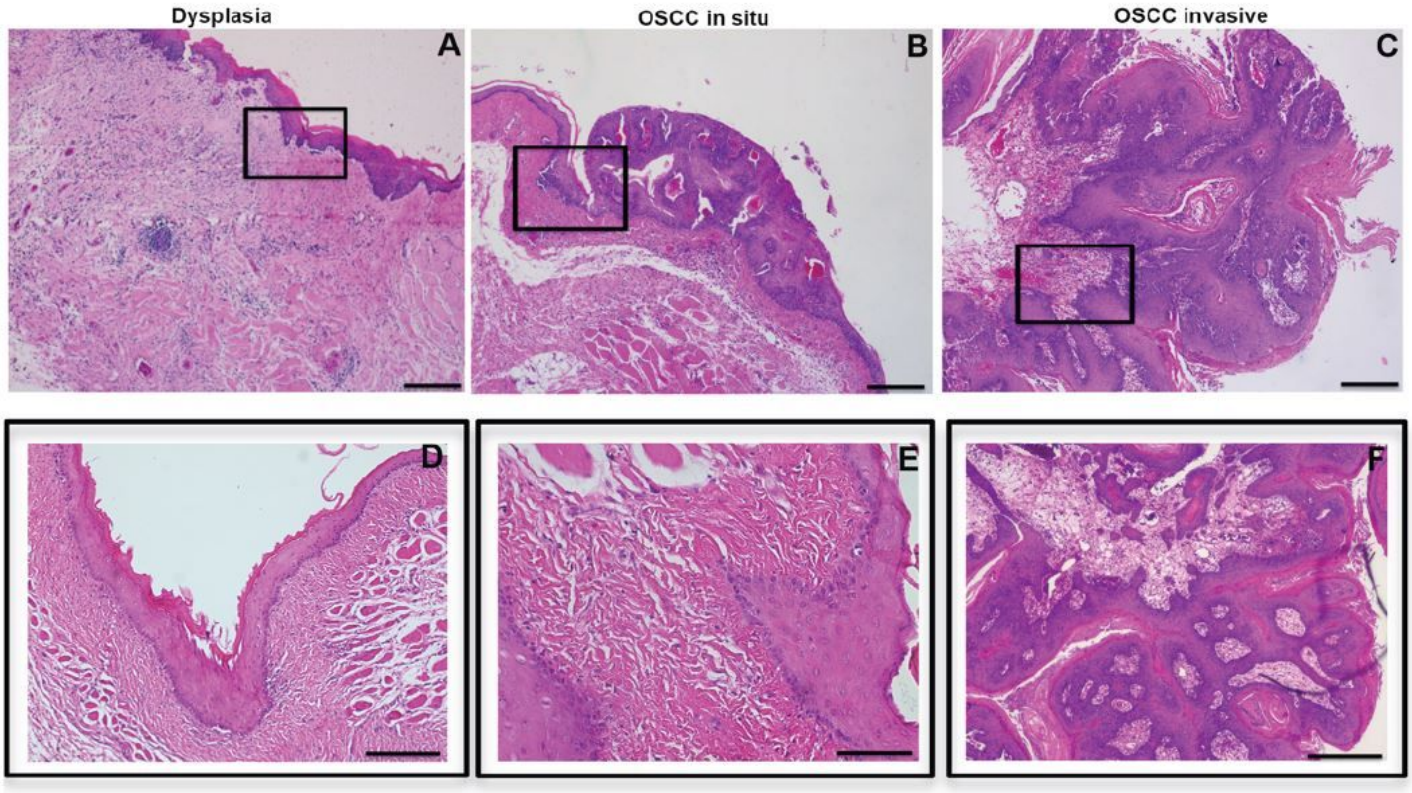

Figure 1

OSCC stages H&E analysis. Oral biopsies of patients were analyzed by H&E and classified into dysplasia (Figures 1A and 1D), less invasive OSCC (Figures 1B and 1E) and highly invasive OSCC (Figures 1C and 1F) according to the changes in the epithelium. The Figures 1A and 1D shown that in all dysplasia cases at different magnification. Regarding the tissue did not show loss of basal membrane continuity or presence of epithelial cells invading the stroma, although an increase in epithelial cell layers and presence of mild leukocyte infiltrate was observed. The biopsies of patients with OSCC both less (Figures 1B and 1 515 E) and highly invasive cases (Figures 1C and 1F), showed at different magnification more than 5 layers of epithelial cells, hyperchromatism, presence of keratin pearls, loss of continuity of the basement membrane and severe leukocyte infiltrate were seen. In the highly invasive OSCC group, epithelial cell nests were observed in the stroma and severe epithelium disorganization, accompanied of leucocyte infiltration of high grade (Figures 1C-F).

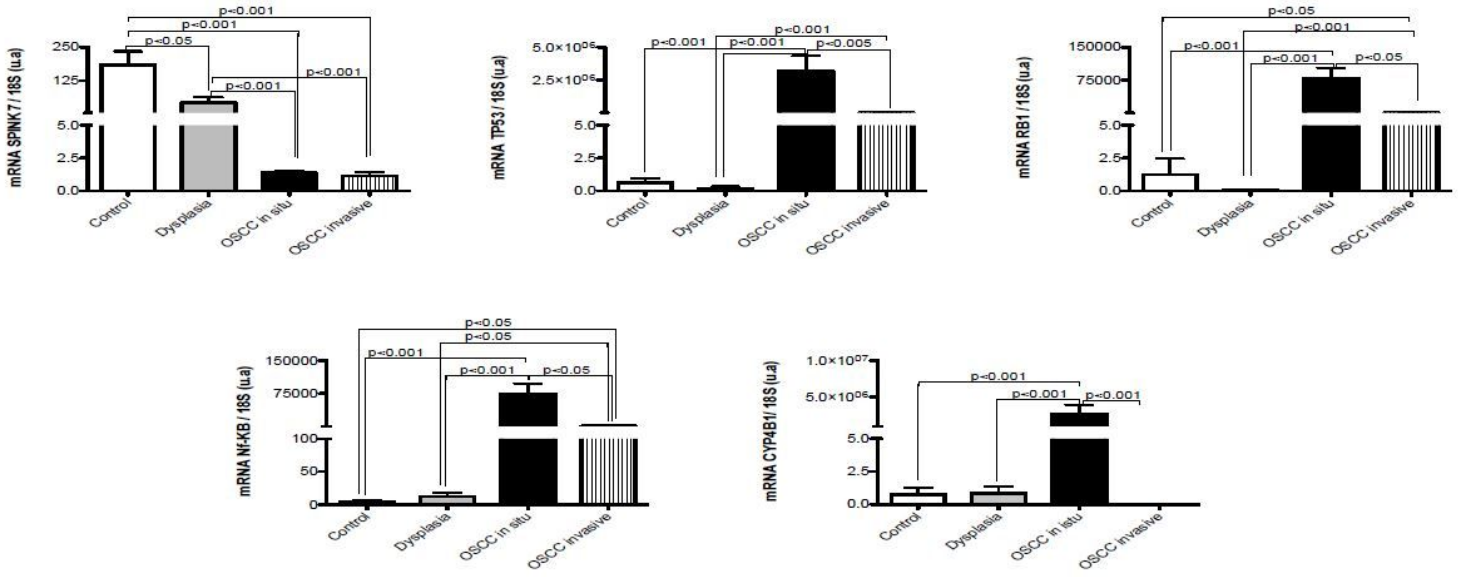

Figure 2

SPINK7, TP53, RB1, NFKB and CYP4B1 gene expression change among the OSCC stages. The graph bar showed the gene expression evaluated by qPCR of each group (normal, dysplasia, less invasive and highly invasive OSCC) and the results were expressed as arbitrary units. The differences were considered statistically significance with P values of (*P<0.05, **P<0.01 and ***P<0.001).

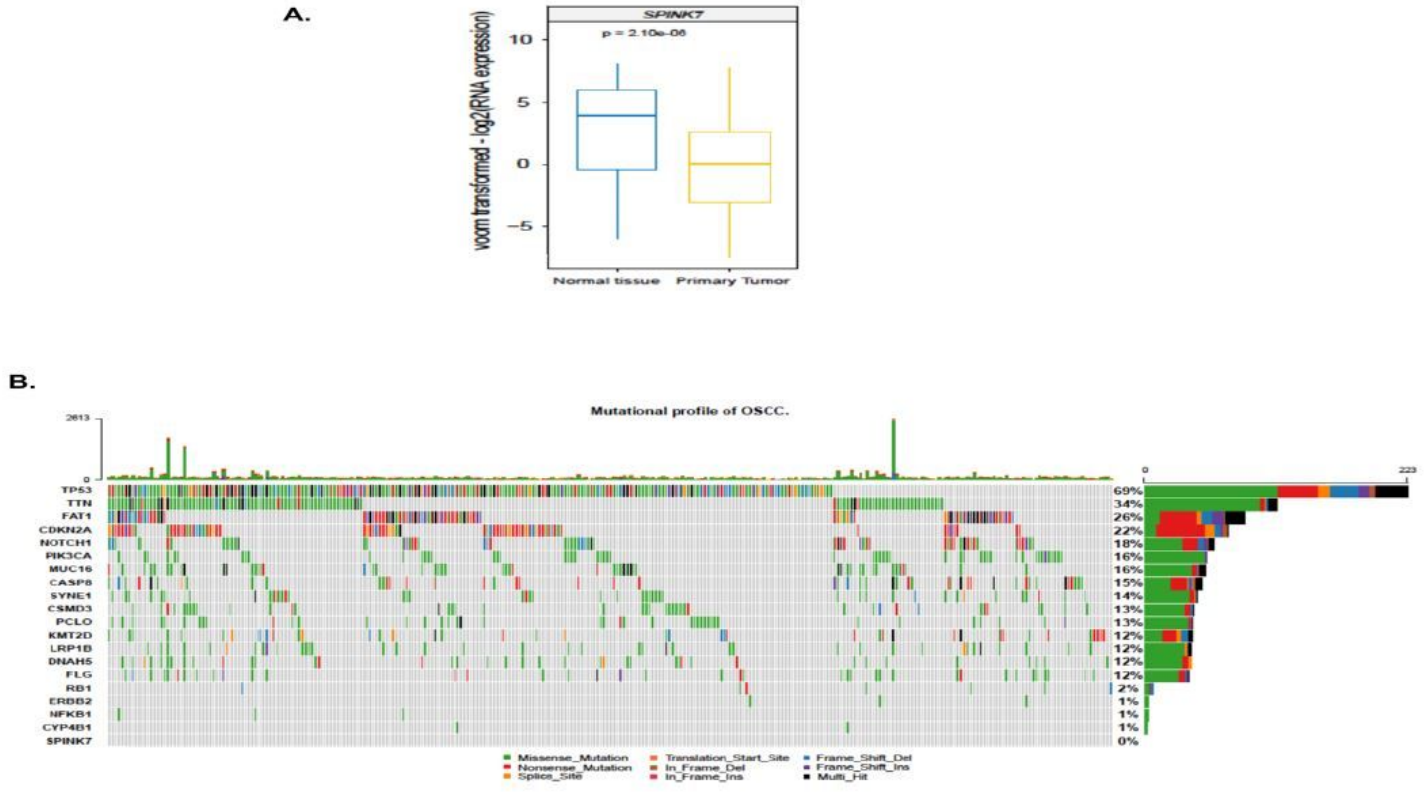

Figure 3

SPINK7 gene expression and mutational profile in a cohort of patients from the TCGA database. A) Box-plot derived of TCGA gene expression analysis of SPINK7 from 581 samples of normal group (box-plot blue) vs primary tumors group (box-plot yellow). B) The Oncoplot graph shows the profile of oral cancer mutations taking into account the fifteen genes with the highest number of mutations (SNP) followed by five genes of interest (RB1, ERBB2/HER2, NFKB1, CYP4B1 and SPINK7). Each column represents a sample of oral cancer and each color represents a type of mutation variant. On the right, the size of each bar represents the frequency of mutations throughout all samples and the percentage of samples that have this mutated gene. Variants annotated as Multi_Hit are those genes that are mutated more than once in the same sample. In the upper part the number of mutations that each sample has graphed.

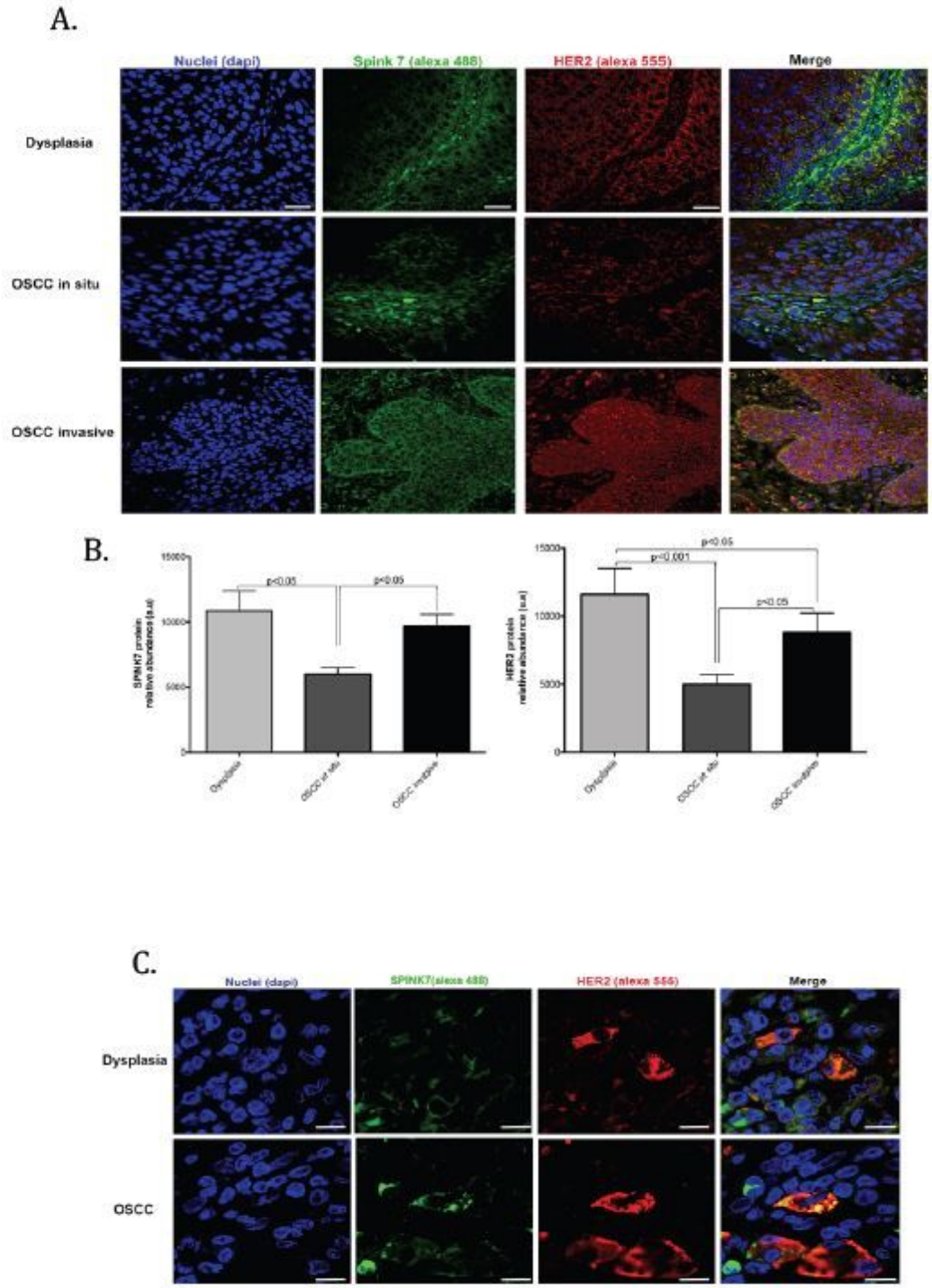

Figure 4

SPINK7 and HER2 proteins analysis among the OSCC stages. A) Immunohistofluorescence of SPINK7 (green) and HER2 (red) proteins evaluated in biopsies of dysplasia, less invasive and highly invasive OSCC. Nuclei were stained with Dapi (blue). The Figure 4B show the graphs bar of the quantitative analysis of pixels intensity (green=SPINK7 and red=HER2) assessed by Image J. The Figure 4C) show the images at high magnification (120X) among the OSCC stages, showing the close localization of both

proteins' signals through overlap image (yellow pixels), Representative images by group, n=6. White bar = 50 µm. The differences were considered statistically significance with P values of (*P<0.05 and ***P<0.001).

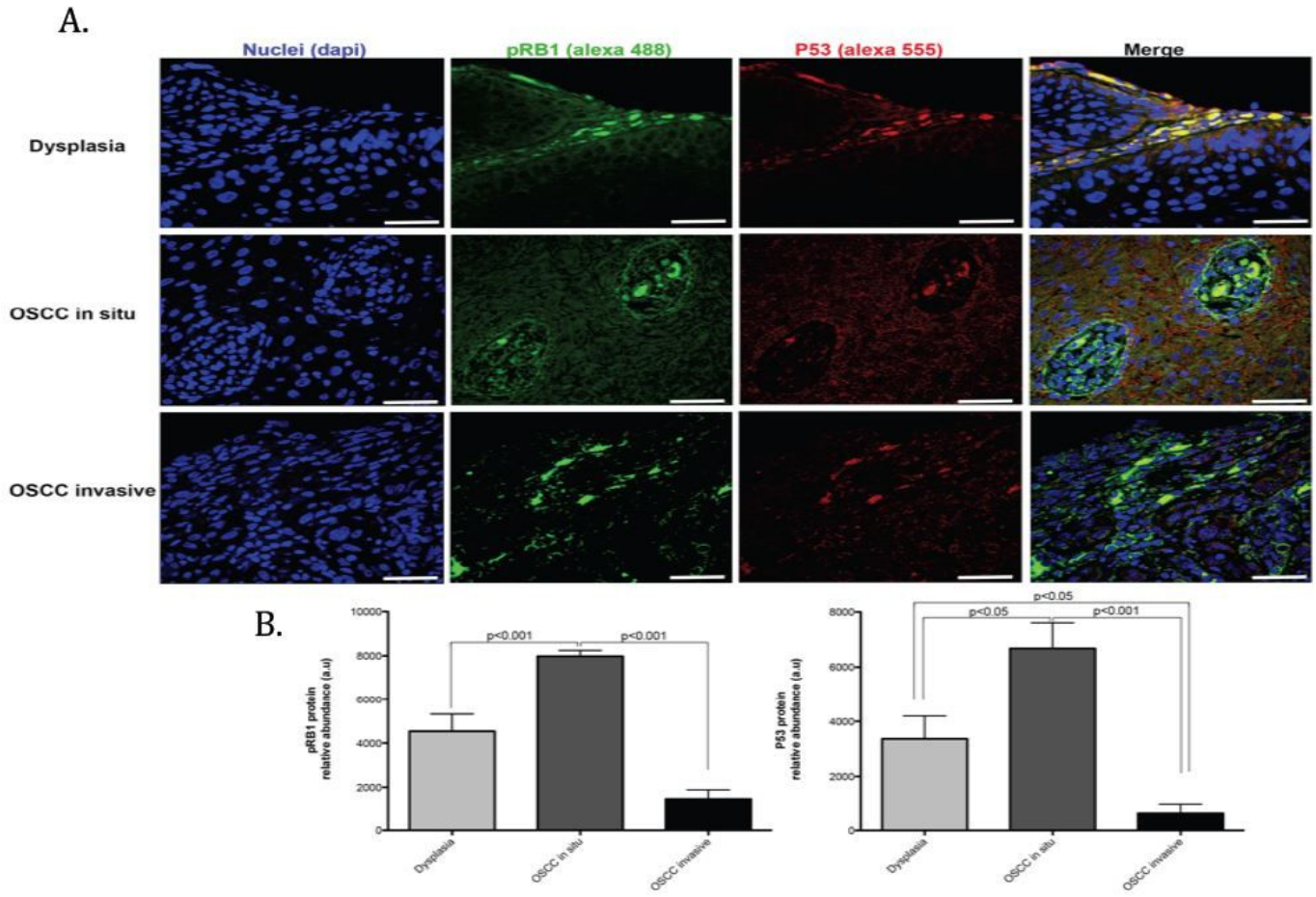

Figure 5

pRB1 and P53 proteins analysis among the OSCC stages. A) Immunohistofluorescence of both proteins, evaluated in biopsies of dysplasia, less invasive and highly invasive OSCC. B) Graphs bar show quantitative analysis of pixels intensity (573 green=pRB1 and red=P53) assessed by ImageJ. Representative images by group, n=6/group. White bar = 50 µm. The differences were considered statistically significance with P values of (*P<0.05 and ***P<0.001).

Supplementary Files

This is a list of supplementary files associated with this preprint. Click to download.

- Pennacchiottietalsupplementarytable.docx